Impact of the Flameholder Heat Conductivity on Combustion Instability Characteristics

Proceedings of ASME Turbo Expo 2012
GT2012
June 11-15, 2012, Copenhagen, Denmark

GT2012-70057

IMPACT OF THE FLAMEHOLDER HEAT CONDUCTIVITY ON COMBUSTION INSTABILITY CHARACTERISTICS

Seunghyuck Hong
Santosh J. Shanbhogue
Ahmed F. Ghoniem*
Reacting Gas Dynamics Laboratory
Center for Energy and Propulsion Research
Department of Mechanical Engeineering
Massachusetts Institute of Technology
Cambridge, Massachusetts 02139

ABSTRACT

In this paper, we investigate the impact of heat transfer between the flame and the flame-holder on the dynamic stability characteristics in a 50-kW backward facing step combustor. We conducted tests where we use a backward step block made of two different materials: ceramic and stainless steel whose thermal conductivities are 1.06 and 12 W/m/K, respectively. A set of experiments was conducted using a propane/air mixture at Re = 6500 for the inlet temperature of 300 − 500 K at atmospheric pressure. We measure the dynamic pressure and flame chemiluminescence to examine distinct stability characteristics using each flame-holder material over a range of operating conditions. We find that for tests with a flame-holder made of ceramic, the onset of instability is significantly delayed in time and, for certain operating conditions, disappears altogether. Stated differently, for certain operating conditions, the combustor can be stabilized by reducing the thermal conductivity of the flame-holder. As the thermal conductivity of the flame-holder increases, the combustor becomes increasingly unstable over a range of operating conditions. These results imply that the dynamic stability characteristics depend strongly on the heat transfer between the flame and the combustor wall near the flame anchoring region.

*Address all correspondence to this author: ghoniem@mit.edu

1 INTRODUCTION

Combustion systems commonly used in gas-turbine engines are susceptible to thermoacoustic instability. As a result of the resonant feedback interactions between the driving heat release mechanisms and the acoustic environment, these combustors are known to exhibit significant pressure and flow oscillations. These oscillations may cause flame extinction and flashback as well as structural vibration and damage. Several mechanisms are known to promote these unsteady coupling processes: e.g., flame-acoustic wave interactions, flame-vortex interactions, equivalence ratio fluctuations, flame-wall interactions and the effect of unsteady stretch rate, which may be present individually or concurrently [1]. Flame-vortex interactions are among the most significant instability mechanisms in large-scale gas turbine combustors [2,3]. When the unsteady heat release rate fluctuations supported by flame-vortex interactions couple positively with the acoustic field, self-sustained acoustic oscillations are observed [4, 5]. The mechanism of flame-vortex interactions has been examined in a number of studies [4–8], where the authors focus on the vortex kinematics (formation, separation and convection) and its interactions with acoustics and the flame.

The role of heat transfer in flame-vortex driven combustion instability has not been as widely studied as the effect of thermal conductivity on the static stability characteristics: that is, lean blow-off or flame flashback. Bollinger and Edse [9] reported their study on the effect of geometric parameters on the burner tip temperature at the moment of flashback in a

bunsen flame. They observed that flashback occurs at a constant burner tip temperature for fuel-lean mixtures, if the thermal conductivity and wall thickness are held constant. Ronney [10] and Khandelwal et al. [11] reported their studies on the effects of thermal conductivity in a micro-scale combustor. The authors demonstrated that the stream-wise conduction through the wall has a significant impact on the operating limit in a micro-scale combustor [10], and that the fabrication of the backward step micro combustor with high thermal conductivity lowers the lean blow-off limit [11]. Khandelwal et al. [11] reported that the micro step combustor made of copper (thermal conductivity = 400 W/m/K) was unable to stabilize the flame within the combustor, because of its high thermal conductivity and resultant high heat loss. Kedia and Ghoniem numerically investigated premixed flame stability characteristics in a perforated plate burner [12], showing the coupled role of heat loss to the burner and the flame curvature on the static flame stabilization and blow-off mechanism. They [13] also demonstrated the critical role of the heat transfer in predicting the dynamic response of the flames to acoustic perturbations.

Triggering of combustion instability has been addressed in the context of the nonlinear nature of thermoacoustic oscillations [14] and non-normality of the system [15, 16]. Lieuwen [14] investigated limit-cycle oscillations in an unstable gas turbine combustor. He demonstrated that the nonlinear characteristics associated with hysteresis in the system's stability boundaries (in which the combustor transitions from stable to unstable operation) is sensitive to background disturbances under stable operating conditions. Balasubramanian et al. [15] and Tulsyan et al. [16] showed that the non-normality in the thermoacoustic system can lead to transient growth in pressure in linearly stable conditions. This, under certain conditions, can lead to high amplitudes oscillations, combined with nonlinear driving, causing the system to become unstable. These two studies investigated the role of acoustics in triggering the instability in the context of the non-normal nature of the system combined with a nonlinear effect in a ducted diffusion flame in a Rijke tube [15] and in a vortex-shedding configuration [16], respectively. Nonetheless, the role of combustion or other thermal processes, e.g., heat transfer, in mode transitions or triggering of the instability has not been studied extensively.

In this paper, we investigate the impact of heat transfer on the dynamic instability characteristics. In particular, we examine the effect of different thermal conductivities at the flame anchoring region on the mode transition from a stable to an unstable operating mode, i.e., the onset of the instability. We report our finding that the onset of the instability can be prevented or significantly delayed by using a material with low thermal conductivity at the flame anchoring region. This study was motivated by our early observation that the onset of the instability is sensitive to the length of time that the combustor operates in the neighborhood of the operating condition that corresponds to the mode transition. We suspect that the heat loss to the combustor wall from the flame is the key mechanism behind this observation. The work presented in this paper summarizes the progress in our effort to elucidate the role of heat transfer in the onset of the instability. Further study on other characteristics of heat transfer at the flame anchoring region is underway for a more quantitative description of the physics.

The rest of the paper is structured as follows: Section 2 describes the combustor configuration, instrumentation and diagnostics as well as the experimental procedure and conditions. In Section 3, we start with the overall stability characteristics of the step combustor, and present the results on our investigation into the effect of using different materials with distinct thermal conductivities at the flame anchoring region. We compare the two cases using stainless steel and ceramic blocks at the flame anchoring region, using the measurements of dynamic pressure and flame chemiluminescence. The paper ends with concluding remarks in Section 4.

2 EXPERIMENTAL SETUP

2.1 Combustor and Diagnostics

Figure 1 shows a diagram of the backward-facing step combustor. The combustor consists of a rectangular stainless steel duct with a cross section 40 mm high and 160 mm wide. The air inlet is choked. At a location 0.45 m downstream from the choke plate, a 0.15 m long ramp reduces the channel height from 40 mm to 20 mm, followed by a 0.4 m long constant area section that ends with a sudden expansion back to 40 mm. The step height is 20 mm. The overall length of the combustor is 5.0 m. A circular exhaust pipe comprises the last 3.0 m of the combustor with a cross sectional area approximately four times that of the rectangular section. The exhaust exits to a trench with a large cross sectional area. Quartz viewing windows installed in the vicinity of the step provide optical access.

An Atlas Copco GA 30 FF air compressor supplies air up to 110 g/s at 883 kPa. A Sierra C100M Smart-Trak digital mass flow controller allows a maximum flow rate of 2.36 g/s for propane. The uncertainty of the flow rate is $\pm 1\%$ of the full scale. Fuel is injected through several spanwise holes in a manifold located 0.96 m upstream of the step, which is 0.02 m downstream of the chock plate. Since the fuel is injected near the chock plate where flow velocity oscillations are weak, the amplitude of equivalence ratio oscillations established at the fuel injector is small. In addition, the distance between the fuel manifold and the step creates a substantial convective delay during which equivalence ratio oscillations are damped as a result of turbulent mixing. In our previous study [8], we demonstrated that the equivalence ratio oscillation is negligible by showing spatial and temporal measurements of equivalence ratio. Air is preheated to a temperature of up to 500 K using an Osram Sylvania 18 kW inline resistive electric heater. The temperature of the inlet mixture is measured using a type K thermocouple mounted 0.2 m upstream of the sudden expansion.

Pressure is measured at three locations: 0.20 m upstream of the sudden expansion and 0.25 m downstream from the beginning of the exhaust pipe using Kulite MIC-093 high intensity microphones mounted in semi-infinite line configurations [17] and 0.15 m downstream of the choke plate using

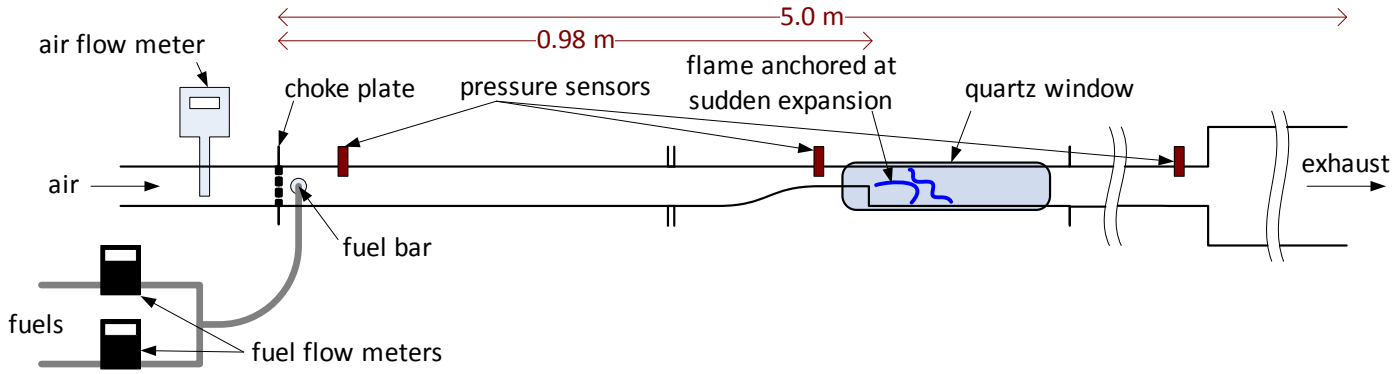

FIGURE 1. SCHEMATIC OF THE BACKWARD-FACING STEP COMBUSTOR WITH INSTRUMENTATION

a flush-mounted, water-cooled Kistler 7061B pressure sensor. High-speed, spatially resolved CH^*-chemiluminescence measurements of the flame at speeds up to 2000 Hz are taken using a NAC GX-1 high-speed CMOS camera with a Nikon 50mm f/1.8 lens. The camera has a resolution of 1280 $\times$ 1024 pixels and a monochrome bit depth of 12 bits per pixel.

All data are acquired using a National Instruments PCIe-6259 data acquisition board and the Matlab Data Acquisition Toolbox. A custom Matlab code is used to store the data and control the experiment.

2.2 Test Setup and Procedure

To investigate the stability characteristics of the combustor, we conducted two series of experiments: equivalence ratio sweep test and transient test. First, we varied the equivalence ratio of the fuel-air mixture either from near stoichiometry toward the lean blow-off limit or from the lean blow-off limit to near stoichiometry, at the inlet temperature of 300 K and 500 K. Equivalence ratio was varied in steps of 0.01 (the flow controllers allow the accuracy of equivalence ratio: $\Delta\phi \sim 0.002$). Pressure response curve as a function of the equivalence ratio are presented in Section 3.1, which identify distinct operating regimes depending on the operating conditions. As shown in Section 3.2, the combustor exhibits strong hysteresis depending on whether the equivalence ratio is increased or decreased.

Second, to further examine the characteristics of the transient behavior while the combustor transitions from the stable regime to the unstable regime, transient tests were conducted at several equivalence ratios in the neighborhood of the operating point at which mode transition occurs. In this series of tests, the equivalence ratio was kept constant either until the combustor exhibits the instability or for 7 minutes if no instability is observed. The rationale behind these tests is based on our observation that the onset of the instability is sensitive to the length of time for which the combustor stays at the constant equivalence ratio, as will be shown in Section 3.3. This is used to show that the heat transfer at the flame anchoring region plays a role in the onset of the instability, as will be discussed in Sections 3.4 and 3.5.

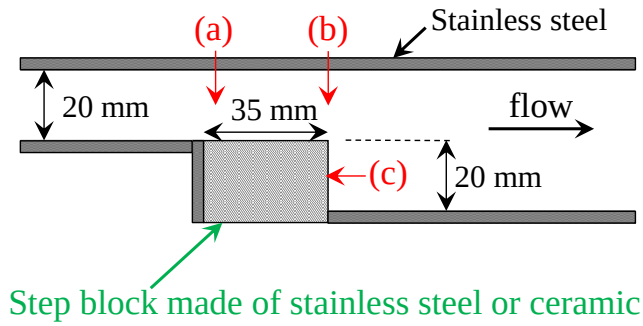

FIGURE 2. SCHEMATIC DIAGRAM SHOWING THE STEP BLOCK MADE OF TWO DIFFERENT MATERIALS INSTALLED IN THE COMBUSTOR. AS SHOWN IN FIGS. 7 AND 8, THE FLAME IS ANCHORED AT THE STEP, (b) OR MOVES ALONG THE WALL BETWEEN (a) AND (b) IF IT FLASHES BACK DURING THE UNSTABLE REGIME. (c) IS WHERE THE BURNED GAS INTERACTS WITH THE WALL, AS WILL BE DISCUSSED IN SECTION 3.5.

The two step blocks were manufactured with stainless steel and ceramic, whose thermal conductivities are 12 W/m/K and 1.06 W/m/K, respectively. The two series of tests described above were conducted with each step block installed at the flame anchoring region (see Fig. 2).

Throughout all tests, the combustor was operated at atmospheric pressure and at the constant Reynolds number of 6500, based on the step height (20 mm). This corresponds to a mean inlet velocity of 5.2 m/s at 300 K, which increases to 12.5 m/s at 500 K. The inlet velocity varies by less than 10% as a function of equivalence ratio.

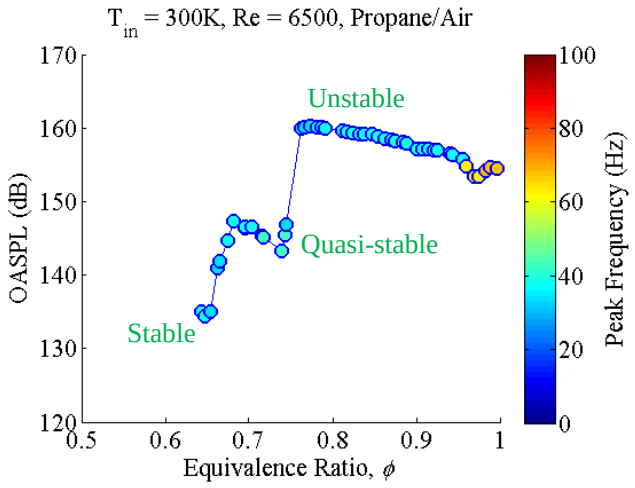

FIGURE 3. OVERALL SOUND PRESSURE LEVEL AS A FUNCTION OF EQUIVALENCE RATIO, SHOWING TYPICAL OPERATING REGIMES: STABLE, QUASI-STABLE AND (LOW FREQUENCY AND HIGH FREQUENCY) UNSTABLE REGIMES. THE COLOR FILLED IN THE MARKERS INDICATES THE PEAK FREQUENCY: $\sim$ 40 Hz IN THE LOW FREQUENCY UNSTABLE REGIME AND $\sim$ 70 Hz IN THE HIGH FREQUENCY UNSTABLE REGIME. A PROPANE/AIR MIXTURE IS USED AT T_{in} = 300 K AND Re = 6500.

3 RESULTS

3.1 Stability Characteristics

The step combustor exhibits several distinct operating regimes depending on the inlet conditions and fuel compositions. Each operating regime can be characterized by the amplitude and frequency of pressure oscillations as well as the flame dynamics. Altay et al. [8] and Speth et al. [18] demonstrated the existence of these operating regimes for propane/hydrogen fuel mixtures and syngas fuel mixtures, respectively, using the pressure measurements and flame chemiluminescence images. In this section, we present the pressure response curve for a propane/fuel mixture to summarize the key characteristics of the operating regimes that will be frequently referred to in the subsequent sections.

Figure 3 shows an overall sound pressure level (OASPL) as a function of equivalence ratio for a propane/air mixture. The OASPL in dB is defined as:

$$\mathrm{OASPL} = 10\log_{10}\left[\overline{\left[\frac{p(t)-\overline{p(t)}}{p_0}\right]^2}\right] \qquad (1)$$

where overbars indicate average values, $p(t)$ is the pressure measured in an interval $t_1 < t < t_2$ and $p_0 = 2\times10^{-5}$ Pa. The pressure sensor close to the sudden expansion (where the flame is anchored) is used for calculating OASPL. Based on the pressure oscillations amplitude, the combustion's operating regimes can be classified into three categories; we refer to those as *stable, quasi-stable and unstable regimes*. As the equivalence ratio is decreased from stoichiometry toward the lean blow-off limit, the combustor transitions from the unstable regimes to the quasi-stable regime, and then to the stable regime, in which the OASPL is 150 $-$ 160 dB, $\sim$ 145 dB and below 140 dB, respectively. Each mode transition occurs if the equivalence ratio is varied beyond a certain threshold. Although not shown here, the combustor exhibits distinct flame dynamics in each operating regime. The main characteristics of the flame dynamics in each operating regime is briefly summarized here (see [8] for the corresponding flame chemiluminescence images in each operating regime, and [19] for the corresponding particle image velocimetry data). In the stable regime, small vortices are shed from the step at a frequency which is not coupled with any acoustic mode of the combustor [20]. The flame is stabilized in a typical reacting shear layer. In the quasi-stable regime, while the flame remains attached to the step, it experiences strong fluctuations at $\sim$ 40 Hz, interacting with the large wake vortex shed from the step. If the combustor transitions to the unstable regimes, the flame strongly interacts with the wake vortex throughout the instability cycle. While the flow exhibits strong fluctuations, the flame detaches from the step during part of each cycle and anchors upstream of the sudden expansion.

In the unstable regimes, we identified two distinct regimes in which the combustor exhibits strong oscillations at two different frequencies: $\sim$ 40 Hz and $\sim$ 70 Hz, as shown in Fig. 3. According to the one dimensional acoustic analysis, although not shown here, the high frequency unstable regime ($\sim$ 70 Hz) corresponds to the fundamental acoustic (1/4-wave) mode, whereas the low frequency unstable regime ($\sim$ 40 Hz) is, as we suspect, associated with an entropy wave mode. The detailed acoustic analysis is described in a parallel study [21]. Within the scope of this study, in which we focus on the mode transition among the stable, quasi-stable and (low frequency) unstable regimes, differentiation between the low frequency- and high frequency- unstable regimes is of no particular importance.

As the inlet temperature and fuel composition are varied, the similar sets of operating regimes described above are observed. The detailed description of those can be found in Refs. [8], [18–20].

3.2 Hysteresis in Mode Transition

Our prior studies [8, 19, 20] demonstrated that the combustor's dynamic modes can be correlated with a variation in strained flame consumption speeds. We showed that numerically-calculated strained flame consumption speed can be used to collapse the combustion dynamics data across full range of equivalence ratios, inlet temperatures and fuel compositions.

In this section, we show that the combustor dynamics also has a strong dependence on the history of the operating regimes, i.e., the presence of hysteresis. Mode transitions, for example, occur at different equivalence ratios depending on

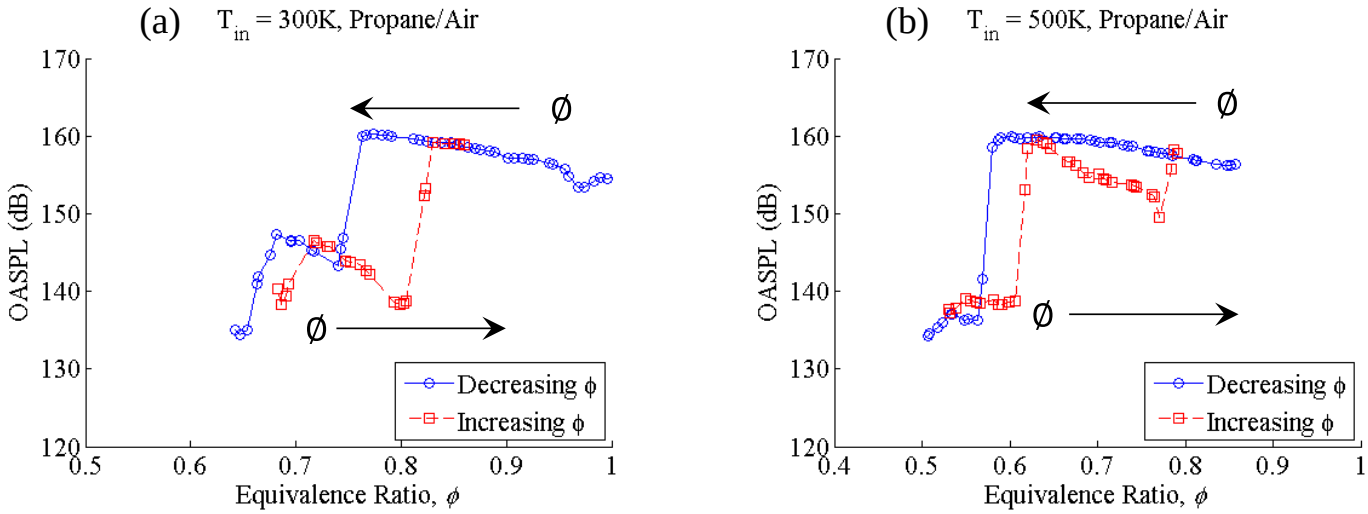

FIGURE 4. OVERALL SOUND PRESSURE LEVEL FOR A PROPANE/AIR MIXTURE AS A FUNCTION OF EQUIVALENCE RATIO, DEMONSTRATING A STRONG HYSTERESIS DEPENDING ON THE HISTORY OF THE EQUIVALENCE RATIO. PRESSURE SIGNALS WERE RECORDED WHILE DECREASING THE EQUIVALENCE RATIO FROM NEAR STOICHIOMETRY TO LEAN BLOW-OFF LIMIT OR INCREASING THE EQUIVALENCE RATIO FROM LEAN BLOW-OFF LIMIT TO NEAR STOICHIOMETRY. A PROPANE/AIR MIXTURE IS USED AT Re = 6500 AND T_{in} = (a) 300 K AND (b) 500 K.

whether the equivalence ratio is decreased from stoichiometry toward lean blow-off limit or increased from near lean blow-off limit toward stoichiometry. Stated differently, although the same sets of operating regimes are observed, the operating point at which the combustor transitions from one regime to another is shifted, as shown in Fig. 4. Similar observations have been reported in a swirl-stabilized combustor for a syngas/air mixture [22] and for a methane/carbon-dioxide/oxygen mixture [23].

In Fig. 4(a), starting at the equivalence ratio near stoichiometry, the combustor operates in the unstable regime for a range of equivalence ratios above a certain threshold ($\phi \approx 0.75$), at which the combustor transitions to the quasi-stable regime. On the other hand, if the equivalence ratio is gradually increased from near lean blow-off limit, the combustor remains in the quasi-stable regime even above $\phi \approx 0.75$, through $\phi \approx 0.80$. This hysteresis phenomenon may be attributed to a nonlinear nature of the combustion system. In the former case (decreasing ϕ), the unstable mode is triggered immediately after "kicking" the equivalence ratio to high enough value near stoichiometry, while in the latter case (increasing ϕ), the combustor transitions to the unstable regime if the equivalence ratio exceeds a certain threshold ($\phi \approx 0.80$). However, the threshold at which the mode transition occurs is not constant depending on whether the combustor load (equivalence ratio) is increased or decreased. This indicates that the operating modes of the combustor depend not only on the operating conditions but also on the history of the state, and that the combustor tends to persist in the present state. As the inlet flow is preheated to 500 K, similar hysteresis phenomenon can be observed in Fig. 4(b), where the mode transition between the unstable and stable regimes occurs at $\phi \approx 0.58$ if the equivalence ratio is decreased, or at $\phi \approx 0.60$ if the equivalence ratio is increased. At the higher inlet temperature, the variation in the critical values of equivalence ratio at which the mode transition is observed decreases to 0.02 ($= 0.6 - 0.58$), compared to 0.05 ($= 0.8 - 0.75$) at 300 K. One possible interpretation is that for the case where the equivalence ratio is increased, if the combustor is initially in a hot state, the combustor transitions from the stable regime to the unstable regime sooner. In this context, it is not clear in the case of increasing ϕ whether the combustor transitioned to the unstable regime because the equivalence ratio exceeded a certain threshold or because the combustor's operating time was long enough to raise the wall temperature near the flame stabilization region, which then promotes the onset of the instability. In the next section, we start from this idea and proceed to the results of transient tests.

3.3 Initial Observation on the Impact of Flame holder Temperature on Time to Instability

While conducting equivalence ratio sweep tests in an ascending order, we observed that the combustor dynamics is sensitive to the length of time for which the combustor stays at the equivalence ratios near the mode transition. To confirm this observation, we conducted a simple test in which we kept the equivalence ratio constant and recorded the time it takes for the onset of the instability. Based on Fig. 4(a), the equivalence ratio was chosen to be $\phi = 0.79$ that is near the mode transition.

The combustor was at room temperature of $\sim$295 K (70 °F, as measured using a radiative thermometer) when a propane/air mixture was ignited. The combustor operated initially in the stable regime. As shown in Fig. 5, the combustor transitioned

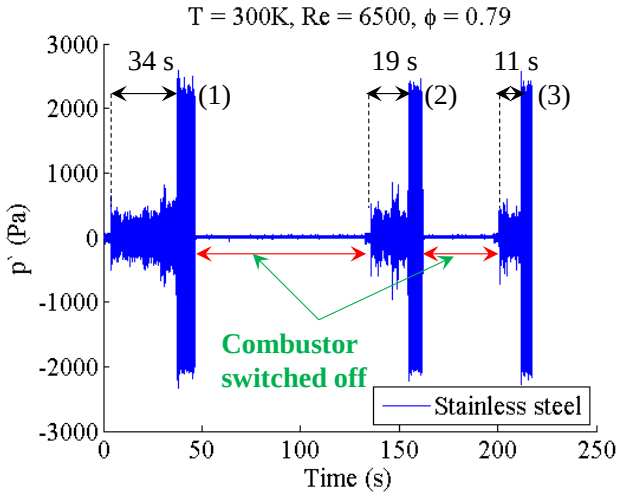

FIGURE 5. A TIME SERIES OF PRESSURE SIGNALS AT $\phi = 0.79$ FOR A PROPANE/AIR MIXTURE, DEMONSTRATING THE EFFECT OF INITIAL WALL TEMPERATURE ON THE ONSET OF THE INSTABILITY. THE COMBUSTOR WAS INITIALLY COLD AT ROOM TEMPERATURE IN CASE (1), WHEREAS IN THE CASES (2) AND (3), THE WALL TEMPERATURE WAS HIGHER AS A RESULT OF CONSECUTIVE OPERATIONS FROM THE CASE (1).

to the unstable regime after 34 seconds. Subsequently after this test, the combustor was ignited again after it had been switched off for ∼90 seconds. The temperature of the step block was ∼317 K (110 °F) at the moment of ignition. In this case, the combustor operated initially in the stable regime, which transitioned to the unstable regime after 19 seconds. The combustor had been switched off for ∼30 seconds after the second test, before it was ignited again. The temperature of the step block at the third ignition was ∼357 K (183 °F). Similarly, the combustor transitioned from the stable regime to the unstable regime after ∼11 seconds. These consecutive tests show that the time it takes until the combustor transitions from the stable to the unstable regime varies depending on the initial temperature of the flame-holder, all other operating conditions being the same. If the temperature of the flame-holder is initially higher, the transition to the unstable regime occurs sooner. This result led us to consider the heat transfer effect on the instability characteristics, as will be discussed in the following sections.

3.4 Impact of Thermal Conductivity on Stability Characteristics

A heat flux depends on several parameters such as heat transfer coefficient, temperature gradient, flow velocity, geometric characteristics. Among these, thermal conductivity (heat transfer coefficient) is determined by the characteristics of the combustor material. In this section, we investigate how different materials with distinct thermal conductivities at the step affect the instability characteristics. The step is where the flame is anchored in all the operating regimes, as shown in the flame chemiluminescence images in [8], and thus the location where the heat transfer between the flame and the combustor wall mainly takes place.

3.4.1 Pressure Response Figure 6 shows OASPL recorded in the equivalence ratio sweep tests with the stainless steel and ceramic blocks. Starting at $\phi = 0.88$, the equivalence ratio was gradually decreased. Since within the scope of this study, we are not particularly interested in the high-frequency unstable regime as described in Section 3.1, the starting point ($\phi = 0.88$) was chosen as to be high enough to trigger the low-frequency instability. At each equivalence ratio, the combustor was operated for $\sim 4-5$ seconds in the stainless steel case and for $\sim 7-8$ seconds in the ceramic case, leading to the total running times of $\sim$ 136 seconds and $\sim$ 238 seconds, respectively. The longer operating time in the ceramic case was intended, as will be discussed later in this section. As seen in Fig. 6, no instability was observed throughout all equivalence ratios in the ceramic case, in which the OASPL remains at 140 dB or lower values, staying in the stable regime, while the instability was observed in the stainless steel case for a range of equivalence ratio ($\phi \geq 0.75$). As the instability was not observed at the beginning ($\phi = 0.88$) in the ceramic case, we operated the combustor for longer time to confirm that the instability is certainly not triggered, based on our observation that the onset of the instability is sensitive to combustor's operating time. However, as will be discussed in Section 3.4.3, if we operate the combustor at one equivalence ratio for much longer time (over several minutes), the instability may eventually be triggered in the ceramic case as well.

3.4.2 Flame Image In this section, we show flame chemiluminescence images for the cases using the stainless steel and ceramic blocks at the step in Figs. 7 and 8, respectively, for the same time period and at the same operating condition: T_{in} = 300 K, Re = 6500 and ϕ = 0.85 for a propane/air mixture. Figure 7 shows a typical sequence of flame images for one instability cycle in the low frequency unstable regime, oscillating at $\sim$ 40 Hz. At the moment of the maximum pressure (1), the vortex starts to form at the step. This is at the moment of the maximum flow acceleration as shown in our prior studies [8, 19]. As the vortex grows and convects downstream (2−6), the flame convolutes itself around the vortex, showing a significant flame-vortex interaction. In the meantime, the reactant packet is formed between the vortex and the burned gas produced in a previous cycle. When the vortex hits the upper wall of the combustor (6), the flame starts to flash back to upstream of sudden expansion. While the flame flashes back (7−8), the combustor experiences intense burning of the reactant packet, exhibiting the maximum heat release rate [8]. The maximum amplitude of pressure fluctuation is $\sim$ 2900 Pa during the cycle. We note here that the flame convoluted around the vortex consistently touches the step block at the moments (2−6), which may heat up the step block. Furthermore, the

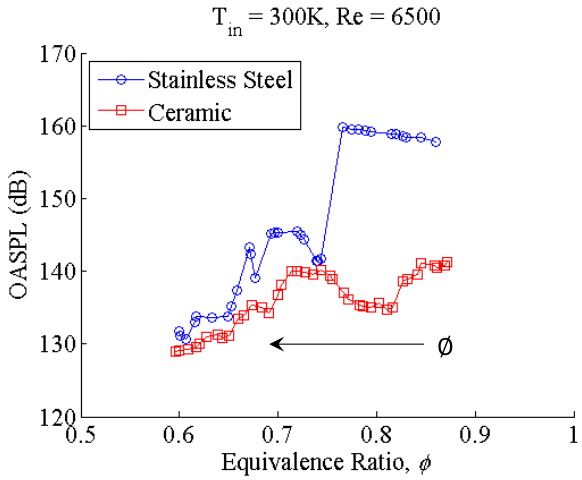

FIGURE 6. OVERALL SOUND PRESSURE LEVEL FOR A PROPANE/AIR MIXTURE AS A FUNCTION OF EQUIVALENCE RATIO. THE TWO DIFFERENT MATERIALS WERE USED AT THE FLAME ANCHORING REGION: STAINLESS STEEL AND CERAMIC. T_{in} = 300 K AND Re = 6500. THE COMBUSTOR'S TOTAL OPERATING TIME IS $\sim$ 136 SECONDS IN THE STAINLESS STEEL CASE AND $\sim$ 238 SECONDS IN THE CERAMIC CASE, RESPECTIVELY.

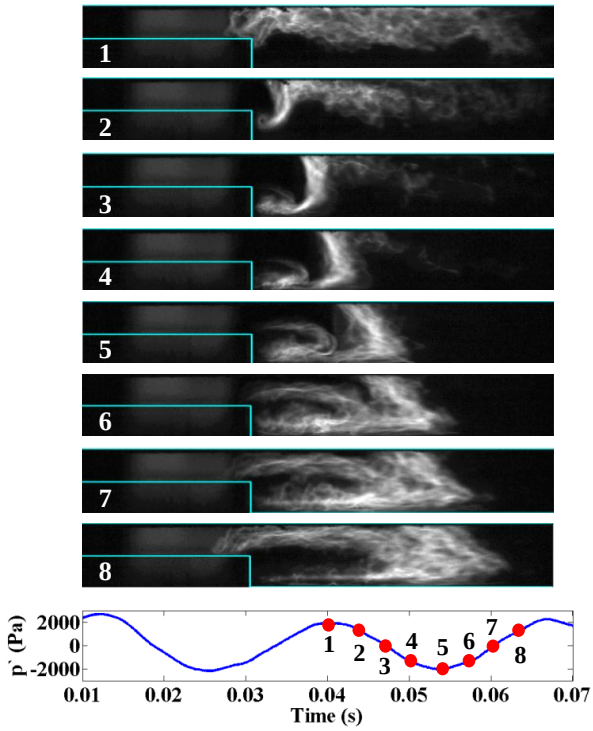

FIGURE 7. A SEQUENCE OF FLAME CHEMILUMINESCENCE IMAGES, WHERE THE STAINLESS STEEL BLOCK IS INSTALLED AT THE STEP. THE COMBUSTOR IS IN THE UNSTABLE REGIME, OSCILLATING AT $\sim$ 40 Hz. THE OPERATING CONDITIONS ARE: ϕ = 0.85, T_{in} = 300 K AND Re = 6500.

strong flow oscillations may enhance the heat transfer significantly. These will be discussed in Section 3.5.

If the ceramic block is used at the step, the maximum amplitude of pressure oscillation is lower at $\sim$ 470 Pa as shown in Fig. 8. We also observe that the flame chemiluminescence intensity (in terms of the brightness of the chemiluminescence image) shown in Fig. 8 is remarkably lower than that in Fig. 7, indicating that the heat release rate oscillation is significantly weaker in the ceramic case. Likewise, the vortex is formed at the step (1 and 5), and convects downstream (2$-$4 and 6$-$8). As the vortex grows and convects downstream, the flame flaps around the vortex, yet still attached to the step. The size of wake vortex while it grows during the cycle is smaller than that in the stainless steel case. The flame dynamics shown in Fig. 8 is similar to that in the quasi-stable regime as shown in [8], in which the flame does not propagate upstream while it interacts with the vortex.

3.4.3 Comparison of Transient Responses As shown in Section 3.4.1, a ceramic block at the flame anchoring region prevents the instability throughout the equivalence ratio sweep test. The physics behind this observation is unknown yet, which will be discussed more in Section 3.5. On the other hand, we also described in Section 3.3 that the onset of the instability is sensitive to the length of time for which the combustor operates at the constant equivalence ratio near the mode transition. Thus, we need an appropriate parameter that reflects these effects on the onset of the instability, and introduce the concept of "*inception time*", defined as the time it takes until the combustor, initially at room temperature before the ignition, transitions from the stable regime to the unstable regime. For example, in Fig. 9, we show a time series of typical pressure fluctuations at ϕ = 0.79. The pressure fluctuates at the amplitude of $\sim$ 500 Pa for the first 90 seconds, corresponding to the stable regime. The amplitude of pressure oscillations suddenly jumps at $\sim$ 95 second, which marks the onset of combustion instability, and hence, the inception time is 95 seconds. In this section, we report a series of tests in which we measure the inception time for several equivalence ratios using the stainless steel and ceramic blocks at the step. If the combustor had remained in the stable regime for 7 minutes, the combustor was switched off. At each equivalence ratio, the test was repeated 3$-$5 times, as will be reported later in this section.

Figures 10 and 11 show the time series of pressure signals recorded at the equivalence ratios of $\phi = 0.78 - 0.81$ using the stainless steel and ceramic blocks at the step, respectively. The pressure signals are plotted against the non-dimensional time, normalized by the instability cycle ($\sim$ 40 Hz) such that it is defined as $t_n = \omega t = 2\pi f t$, where $f \equiv$ 40 Hz; e.g., 1 second corresponds to $t_n \approx 250$. The normalized time allows us to estimate how much time is necessary for the onset of the instability in terms of the number of instability cycles. At $\phi = 0.78$, the combustor has remained in the stable regime for 7 minutes for

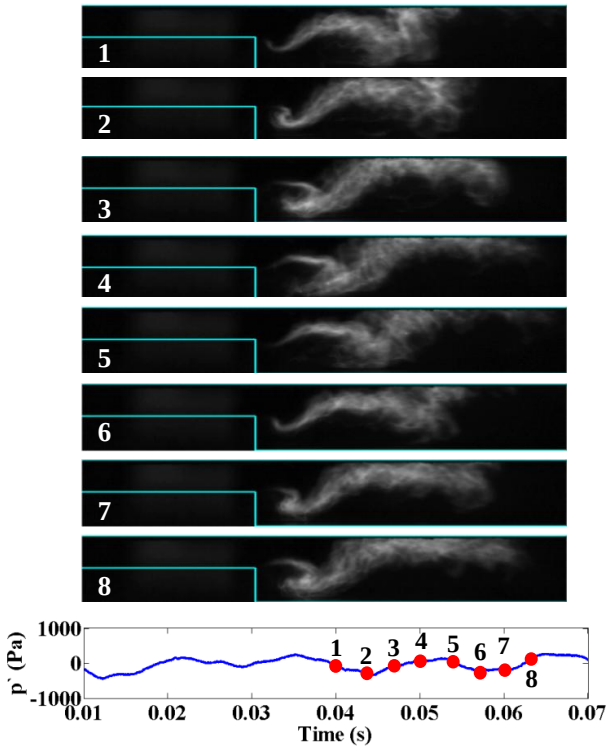

FIGURE 8. A SEQUENCE OF FLAME CHEMILUMINESCENCE IMAGES, WHERE THE CERAMIC BLOCK IS INSTALLED AT THE STEP. THE COMBUSTOR IS STABLE. THE OPERATING CONDITIONS ARE: ϕ = 0.85, T_{in} = 300 K AND Re = 6500.

both cases with the stainless steel and ceramic blocks. As we repeat the tests at higher equivalence ratios (ϕ = 0.79 − 0.81), we observe the difference between the cases with the stainless steel and ceramic blocks. For the cases with the stainless steel block (see Figs. 10(b)−(d)), the combustor transitions from the stable regime to the unstable regime after a certain amount of time at each equivalence ratio. The inception time decreases from $\sim$ 90 seconds to $\sim$ 1 second as the equivalence ratio is raised from $\phi = 0.79$ to $\phi = 0.81$, indicating that the combustor tends to exhibit the instability sooner at higher equivalence ratio. We note here that the mode transition to the unstable regime was also observed at ϕ = 0.80 in the equivalence ratio sweep test (ascending order), as shown in Fig. 4(a).

In contrast, for the case using the ceramic block at the step, the combustor remains in the stable regime for 7 minutes even at $\phi = 0.79 - 0.80$, as shown in Figs. 11(b)−(c). At $\phi = 0.81$, the combustor transitions from the stable regime to the unstable regime after $\sim$ 80 seconds. A comparison between the stainless steel and ceramic cases at $\phi = 0.79 - 0.81$ demonstrates that lower thermal conductivity at the flame anchoring region can successfully prevent the instability (at $\phi = 0.79 - 0.80$) or significantly delay the onset of the instability in time (at $\phi = 0.81$). Similar effect of low thermal conductivity was also shown in the equivalence ratio sweep test (Fig. 6) and in the flame images recorded at $\phi = 0.85$ (Figs. 7 and 8), where the instability was not observed with the use of a ceramic block at the flame anchoring region.

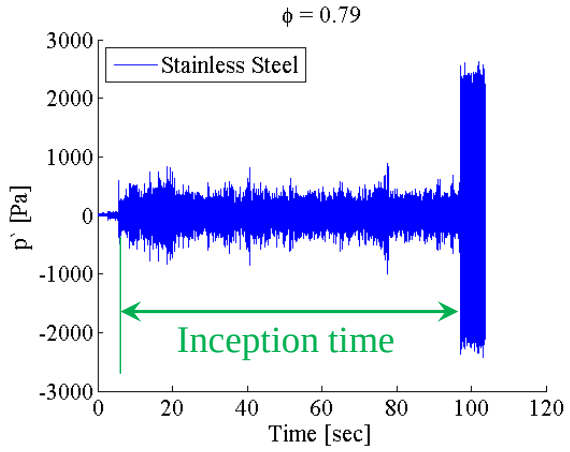

FIGURE 9. A TYPICAL TIME SERIES OF PRESSURE FLUCTUATION IN THE STEP COMBUSTOR. THE EQUIVALENCE RATIO WAS KEPT CONSTANT ($\phi = 0.79$) AT T_{in} = 300 K.

To construct a comprehensive set of data to support the observation described above, we repeated the transient tests at a range of equivalence ratios with the ceramic step block. Figure 12 shows the pressure signals against the non-dimensional time recorded in repeated tests at ϕ = 0.81. As shown in the figure, we observed the intermittent existence of the instability. In the repeated case shown in Fig. 12(b), the combustor transitioned from the stable regime to the unstable regime after $\sim$ 46 seconds, which occurred earlier than the first test shown in Fig. 12(a). However, the combustor transitioned back to the stable regime after $\sim$ 4 seconds, remaining there for the next $\sim$ 30 seconds. The combustor exhibited the instability intermittently until the instability was observed consistently, after $\sim$ 390 seconds ($t_n \approx 9.75 \times 10^4$), indicating that the flame prefers to be in the stable regime even after the instability is triggered. Although not shown here, the combustor exhibited this intermittent instability at several equivalence ratios in repeated tests using the ceramic block, while this behavior of *being intermittently unstable* had never been observed in the stainless steel cases in which the combustor was always *robustly unstable* once it transitioned to the unstable regime. This confirms in a broad sense that the heat transfer through the combustor wall at the flame anchoring region plays a role in the combustion instability, as will be discussed in the next section.

In Fig. 13, we show the inception times measured over a range of equivalence ratios using the two materials. If the combustor is intermittently unstable for some time, we measure the inception time as the time after which the combustor remains consistently in the unstable regime. The error bars are plotted to show the variance of inception times measured in repeated tests. The overall trend shows larger inception time for the cases with the ceramic block, which indicates that the on-

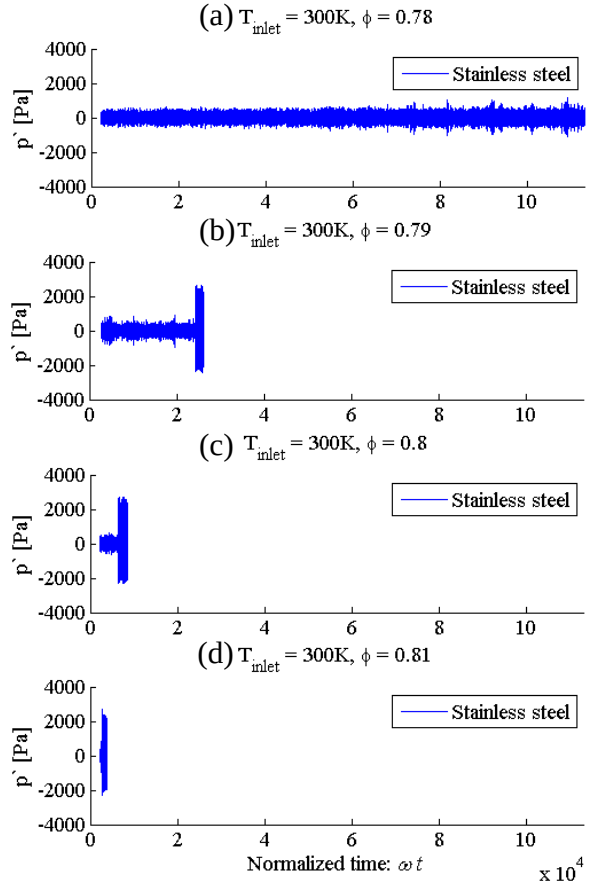

FIGURE 10. A SET OF TIME SERIES OF PRESSURE SIGNALS IN THE STEP COMBUSTOR USING THE STAINLESS STEEL BLOCK AT THE FLAME ANCHORING REGION, AT $\phi = 0.78 - 0.81$.

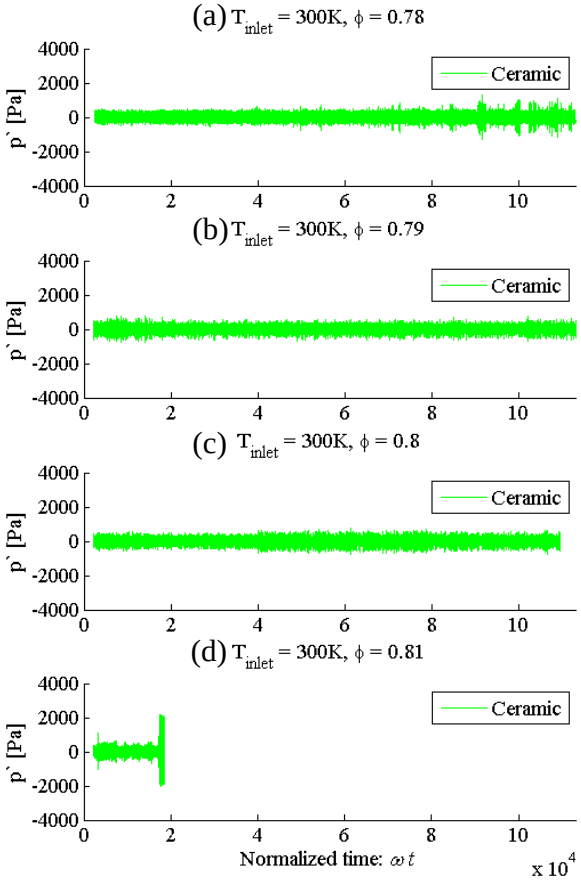

FIGURE 11. A SET OF TIME SERIES OF PRESSURE SIGNALS IN THE STEP COMBUSTOR USING THE CERAMIC BLOCK AT THE FLAME ANCHORING REGION, AT $\phi = 0.78 - 0.81$.

set of the instability can be significantly delayed in time over a range of equivalence ratio with the use of ceramic block at the flame anchoring region. The cases with the ceramic block show larger variance, mainly attributed to being intermittently stable and unstable, as described above (note the log scale in y-axis in Fig. 13). At $\phi = 0.79 - 0.80$, the combustor with the ceramic block did not exhibit any instability for the test running time (7 minutes) in the repeated tests, whereas the combustor transitioned from the stable to the unstable regime with the stainless steel block within $\sim$ 1 minute. Given that the combustor was operated in each test for 7 minutes at most, these results indicate that the use of ceramic block at the flame anchoring region can expand the stability margin to higher equivalence ratio at least for certain amount of time. In the next section, we suggest a possible mechanism underlying our observations on the effect of lower thermal conductivity on preventing or delaying the onset of the instability.

3.5 Discussion

In prior studies by our research group [8, 19, 20, 22, 24], we demonstrated that the operating regimes and the mode transitions can be correlated with the strained flame consumption speed. The numerically-calculated strained flame consumption speed, as a function of the fuel composition, inlet temperature and equivalence ratio, was used to collapse combustion dynamics data across the full range of operating conditions. This was shown to work well for both the step [8, 19, 20] and the swirl-stabilized [20, 22, 24] combustors using propane/hydrogen fuel mixtures and syngas fuel mixtures. We showed that the mode transition from the stable to the unstable regime occurs at a critical value of strained flame speed. Stated differently, the flame speed must be higher than a certain threshold in order for the combustor to become unstable. In addition, we showed that the mode transition shifts to lower equivalence ratio with higher concentration of hydrogen in a syngas fuel mixture [18–20], indicating that higher flame speed leads the combustor to be more readily unstable at leaner conditions. In this section, we discuss qualitatively the experimental observations described in the preceding sections, in the context of the flame speed and

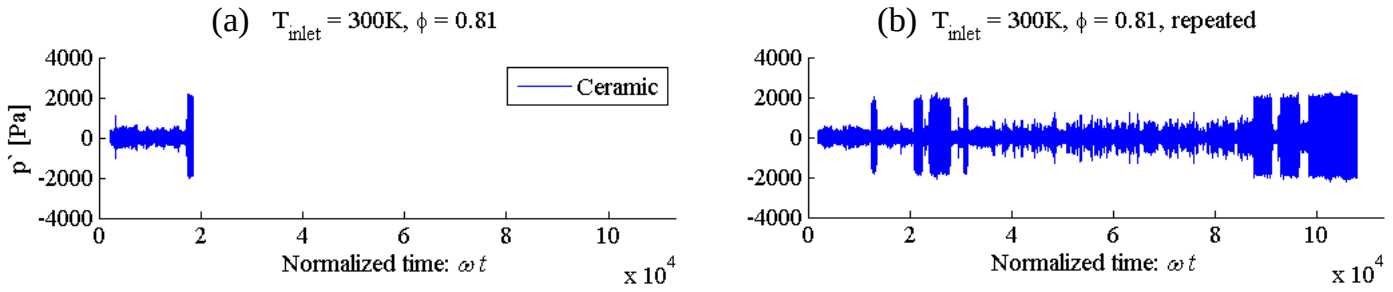

FIGURE 12. TIME SERIES OF PRESSURE SIGNALS FROM THE SET OF REPEATED TESTS USING THE CERAMIC BLOCK AT THE FLAME ANCHORING REGION AT $\phi = 0.81$, DEMONSTRATING THE INTERMITTENT EXISTENCE OF THE INSTABILITY.

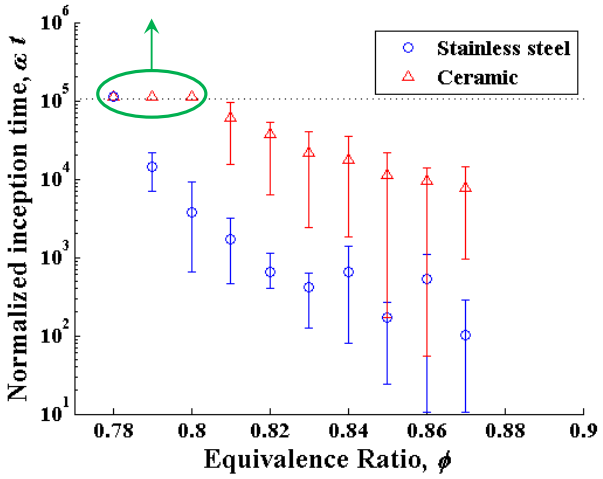

FIGURE 13. NORMALIZED INCEPTION TIMES AT A RANGE OF EQUIVALENCE RATIOS, TESTED WITH TWO DIFFERENT MATERIALS AT THE FLAME ANCHORING REGION. THE MARKERS IN A GREEN CIRCLE INDICATE THE CASES IN WHICH THE COMBUSTOR DID NOT EXHIBIT THE INSTABILITY FOR 7 MINUTES.

its dependence on the local reactants temperature. Naturally, additional investigation into the role of heat transfer will be pursued in the future for a more quantitative analysis.

The results shown in Section 3.4 indicate that the use of a material with low thermal conductivity at the flame anchoring region can expand the stability margin in equivalence ratio or significantly delay the onset of the instability in time. Considering the current setup as shown in Fig. 2, the flame is either anchored at (b), or moving between (a) and (b) during the instability cycle, as seen in Fig. 7. Heat can be transferred by conduction through the step block from the burned gas to the combustor wall along the surface (c) in Fig. 2 if the flame is anchored at (b), or by the same mechanism plus convection between the two points (a) and (b) during the cyclic flame motion (flashback). In the latter case, the cyclic motion of the flame along the wall can heat it up while the flame is moving upstream, and that heat is convected back to the fresh mixture.

Now, consider the two cases in which the combustor is initially in a hot or cold state, using the stainless steel block at the step (see the case shown in Fig. 5 and described in Section 3.3). If the combustor is initially hot, it transitions from the stable regime to the unstable regime faster, as shown in Fig. 5. This can be explained as follows. Higher wall temperature along the step block between (a) and (b) in Fig. 2 enhances the preheating of the incoming fresh mixture in the low velocity region near the wall. Given that the flame is anchored at the step (b), the preheated reactants raise the flame speed near the wall (the low velocity region), where the flame is anchored. This can, under some conditions, help the flame move away upstream along the wall (flashback). In summary, high wall temperature near the flame anchoring region preheats the incoming fresh mixture near the wall, raising the flame speed, and promoting the motion of the flame upstream (flashback).

The same idea can be applied to the comparison between the cases with the stainless steel and ceramic blocks. Consider the cases at the same equivalence ratio, $\phi = 0.85$, shown in Figs. 7 and 8. Given that the combustor is initially at room temperature in both cases (and all other operating conditions are the same), different thermal conductivities should play a role in differentiating the two cases. We start with the stainless steel case. In Fig. 7, we observe that while the vortex grows in size, the burned gas trapped in the wake region consistently exists immediately downstream of the step, i.e., at (c) in Fig. 2. Therefore, the burned gas heats up the wall at (c). Heat conduction through the step block from (c) to (a) contributes to preheating the incoming fresh mixture in the low velocity region near the wall, hence raising the speed of the flame near the wall (in the low velocity region) where it is anchored. This strengthens the flame, and promotes the flame to propagate upstream, contributing to the onset of the instability. In contrast, as seen in Fig. 8, the flame convoluted around the vortex stays further downstream of the step in the less conducting ceramic case, which suggests that there is less contribution to heating the wall at (c) (in Fig. 2) than that in the stainless steel case, where the burned gas consistently touches the step block as shown in Fig. 7. Furthermore, lower thermal conductivity results in less heat flux through the step block from (c) to (a) in the ceramic case. Therefore, there is less contribution to the

preheating of the fresh mixture, and thus the flame speed at the flame anchoring region is not raised as much as in the stainless steel case. As a result, the onset of the instability is prevented or significantly delayed.

Next, we consider the case where the flame flashes back along the wall from (b) to (a) (in Fig. 2). During the flashback, a significant velocity oscillation causes the flow in the reverse direction [19]. At these moments, heat is transferred from the burned gas (under the flame) to the wall region between (a) and (b). Given the lower thermal conductivity of the ceramic, the penetration depth of the heat by conduction is smaller in the ceramic case, hence reducing the heat convected back (by the flow in the reverse direction) to the fresh mixture because of the lower temperature on the step block. The lower temperature along the wall upstream of the step also leads to less preheating of the fresh mixture near the wall in the low velocity region, as discussed above. These combined effects can not maintain the flame speed high enough to sustain the instability after a number of instability cycles. The flame then moves downstream, and is anchored at the step, indicating that the combustor transitions back to the stable regime. In contrast, the heating of the step block (through (a)−(c) in Fig. 2) is enhanced in the stainless steel case because of its high thermal conductivity. This explains the observation made earlier that the combustor switches back and forth between stable and unstable behaviors in the tests with the ceramic block. We plan to measure the temperature along the wall near the flame anchoring region to support the discussion in this section.

4 CONCLUDING REMARKS

In this paper, we investigated the impact of different thermal conductivities on the dynamic stability characteristics for a propane/air mixture over a range of operating conditions. We report our observation that the instability in the step combustor is sensitive to an initial temperature of the combustor wall near the flame stabilization region. Starting from this observation, we examined the role of heat transfer in the onset of the instability, using the two materials with distinct thermal conductivities −stainless steel and ceramic− at the flame anchoring region. The experimental results suggest that using blocks of ceramic, low heat conducting materials of certain geometry and strategically located in the flame anchoring region, provides passive dynamics suppression approach over a wide range of operating conditions.

For the case with the stainless steel block, the combustor exhibits a robust instability for a range of operating conditions. In contrast, for the case with the ceramic block, the instability can be prevented or significantly delayed over a range of equivalence ratio. Furthermore, the instability, even after it is triggered, is not robust, and the combustor tends to operate in the stable regime, exhibiting intermittent transitions between the stable and the unstable regimes. We suggest a possible mechanism behind this phenomenon in the context of a heat transfer and a resultant variation in flame speeds.

In the future, we plan to measure the temperature on the combustor wall near the flame anchoring region and examine the effect of other parameters that may affect the heat transfer, for a more quantitative description of the physics.

ACKNOWLEDGMENT

The authors would like to acknowledge the King Abdullah University of Science and Technology for their support of this research. This work was funded by the KAUST grant, number KUS-110-010-01.

REFERENCES

[1] Ducruix, S., Schuller, T., Durox, D., and Candel, S., 2003. "Combustion dynamics and instabilities: elementary coupling and driving mechanisms". *Journal of Propulsion and Power,* ***19***(5).

[2] Venkataraman, K. K., Lee, B. J., Preston, L. H., Simons, D. W., Lee, J. G., and Santavicca, D. A., 1999. "Mechanism of combustion instability in a lean premixed dump combustor". *Journal of Propulsion and Power,* ***15***(6), pp. 909–918.

[3] Bernier, D., Lacas, F., and Candel, S., 2004. "Instability mechanisms in a premixed prevaporized combustor". *Journal of Propulsion and Power,* ***20***(4), pp. 648–656.

[4] Poinsot, T. J., Trouve, A. C., Veynante, D. P., Candel, S. M., and Esposito, E. J., 1987. "Vortex driven acoustically coupled combustion instability". *Journal of Fluid Mechanics,* ***177***, pp. 265–292.

[5] Ghoniem, A. F., Park, S., Wachsman, A., Annaswamy, A. M., Wee, D., and Altay, H., 2005. "Mechanism of combustion dynamics in a backward-facing step stabilized premixed flame". *Proceedings of the Combustion Institute,* ***30***, pp. 1783–1790.

[6] Yu, K. H., Trouve, A., and Daily, J. W., 1991. "Low-frequency pressure oscillations in a model ramjet combustor". *Journal of Fluid Mechanics,* ***232***, pp. 47–72.

[7] Matveev, K. I., and Culick, F. E. C., 2003. "A model for combustion instability involving vortex shedding". *Combusion Science and Technology,* ***175***, pp. 1059–1083.

[8] Altay, H. M., Speth, R. L., Hudgins, D. E., and Ghoniem, A. F., 2009. "Flame-vortex interaction driven combustion dynamics in a backward-facing step combustor". *Combustion and Flame,* ***156***, pp. 1111–1125.

[9] Bollinger, L. E., and Edse, R., 1956. "Effect of burner-tip temperature on flash back of turbulent hydrogen-oxygen flames". *Industrial and Engineering Chemistry,* ***48***(4), pp. 802–807.

[10] Ronney, P. D., 2003. "Analysis of non-adiabatic heat-recirculating combustors". *Combustion and Flame,* ***135***(4), pp. 421–439.

[11] Khandelwal, B., Sahota, G. P. S., and Kumar, S., 2010. "Investigations into the flame stability limits in a backward step micro scale combustor with premixed methane-air mixtures". *Journal of Micromechanics and Microengineering,* ***20***(9), pp. 1–8.

[12] Kedia, K. S., and Ghoniem, A. F., 2011. "Mechanisms of stabilization and blowoff of a premixed flame downstream of a heat-conducting perforated plate". *Combustion and Flame,* ***159***(3), pp. 1055–1069.

[13] Kedia, K. S., Altay, H. M., and Ghoniem, A. F., 2011. "Impact of flame-wall interaction on flame dynamics and transfer function characteristics". *Proc. Combust. Inst.,* ***33***, pp. 1113–1120.

[14] Lieuwen, T. C., 2002. "Experimental investigation of limit-cycle oscillations in an unstable gas turbine combustor". *Journal of Propulsion and Power,* ***18***(1), pp. 61–67.

[15] Balasubramanian, K., and Sujith, R. I., 2008. "Thermoacoustic instability in a Rijke tube: Non-normality and nonlinearity". *Physics of Fluids,* ***20***(4).

[16] Tulsyan, B., Balasubramanian, K., and Sujith, R. I., 2009. "Revisiting a model for combustion instability involving vortex shedding". *Physics of Fluids,* ***181***(3), pp. 457–482.

[17] Englund, D., and Richards, W. B., 1984. *The infinite line pressure probe*. Technical Report NASA TM-83582, National Aeronautics and Space Administration.

[18] Speth, R. L., Altay, H. M., Hudgins, D. E., and Ghoniem, A. F., 2007. "Dynamics and stability limits of syngas combustion in a backward-facing step combustor". *Proceedings of ASME Turbo Expo*(GT2007-28130).

[19] Speth, R. L., Hong, S., Shanbhogue, S. J., and Ghoniem, A. F., 2011. "Mode selection in flame-vortex driven combustion instabilities". *49th AIAA Aerospace Sciences Meeting*(2011-236).

[20] Speth, R. L., Altay, H. M., Hudgins, D. E., Annaswamy, A. M., and Ghoniem, A. F., 2008. "Vortex-driven combustion instabilities in step and swirl-stabilized combustors". *46th AIAA Aerospace Sciences Meeting and Exhibit*(2008-1053).

[21] Hong, S., Speth, R. L., Shanbhogue, S. J., and Ghoniem, A. F., 2012. "Experimental study and modeling analysis of mode selection in flame-vortex driven combustion instabilities". *in preparation*.

[22] Speth, R. L., 2010. "Fundamental studies in hydrogen-rich combustion: Instability mechanisms and dynamic mode selection". PhD thesis, Massachusetts Institute of Technology.

[23] Shroll, A. P., Shanbhogue, S. J., and Ghoniem, A. F., 2011. "Dynamic-stability characteristics of premixed methane oxy-combustion". *Proceedings of ASME Turbo Expo*(GT2011-45753).

[24] Speth, R. L., and Ghoniem, A. F., 2009. "Using a strained flame model to collapse dynamic mode data in a swirl-stabilized syngas combustor". *Proceedings of the Combustion Institute,* ***32***, pp. 2993–3000.